

Depassivation–repassivation Behavior of a CoCrMo Alloy under Tribological Contact in Simulated Body Fluids

Xinyi Li¹, Yu Yan^{1,*}, Haijun Zhang², Yanjing Su¹, Lijie Qiao¹

¹ Corrosion and Protection Center, Key Laboratory for Environmental Fracture (MOE), Institute of Advanced Materials and Technology, University of Science and Technology Beijing, Beijing 100083, P.R.China

² Shandong Rientech Medical Tech Co., Ltd., Branden Industrial Park, Qihe Economic & Development Zone, 251100, Qihe, Shandong Province, P.R. China

*E-mail: yanyu@ustb.edu.cn

Received: 5 January 2017 / Accepted: 30 January 2017 / Published: 12 February 2017

The long term performance of CoCrMo alloys in a tribocorrosive environment relies on the passivation properties of such alloys. The depassivation–repassivation phenomenon of CoCrMo alloy surfaces in a 0.9% NaCl solution, with and without the addition of Bovine Serum Albumin (BSA), was investigated. The relationships between the wear-induced-depassivation rate (D), applied load (F) and stroke frequency (f) were deduced. These can be summarised as $D = 7.57E-6F^{0.56}f$ in a 0.9% NaCl solution and $D = 2.31E-6F^{0.85}f$ in BSA containing solution. It was found that the ratio of the Cr element in the outer layer of the passive film was lower after depassivation. The passive film formed initially has better stability, which results in a lower depassivation rate in the initial few cycles compared with later cycles (relatively stable) in 0.9% NaCl solution. The adsorption of BSA and the effects of mechanical wear result in a higher depassivation rate in the initial a couple of cycles in BAS containing 0.9% NaCl solution.

Keywords: tribocorrosion; depassivation; repassivation

1. INTRODUCTION

Corrosion and wear resistance are the two important factors affecting the service life of alloys, and the interaction of tribology and corrosion in aqueous sliding conditions was studied [1, 2]. The key point in the tribocorrosion process is depassivation–repassivation behaviour. Depassivation is defined as an increase in corrosion current caused by the change of passive film properties, which mainly include composition, structure, thickness, electrical conductivity etc. Some authors have used mechanical, chemical and electrochemical methods to destroy passive film in order to achieve

depassivation. Fushimi [3] investigated the depassivation–repassivation of iron surfaces in boric–borate solutions using a micro-indentation test and pointed out that plastic deformation of the surface was accompanied by surface depassivation, while no depassivation occurred during elastic deformation. Nano-indentation tests were performed to examine the nano-mechano-electrochemical properties of passive film formed on titanium [4] and iron [5, 6] surfaces in solution or air. Ghods [7] showed that the addition of chloride to the CP solution could lead to the breakdown of passive film on carbon steel and change its composition and thickness. Hodgson [8] used electrochemical techniques to study passive and transpassive behavior of CoCrMo alloys in simulated body fluids. It was found that the oxide film is enriched with Cr during the activation/repassivation cycles, while active dissolution is mainly dominated by the alloying element Co. Landolt [9] proposed a proportional relationship between anodic current enhancement and mechanical parameters, such as the applied load and sliding speed of the tribocorrosion process.

Repassivation capability is an important factor influencing corrosion resistance when the passive film is broken [10]. High Field conduction Models (HFM) and InterFace Models (IFM) were put forward to predict film growth models [11]. Repassivation of a wear scar showed that the initial growth of the passive film is controlled by ion migration in a high electric field obeying an inverse logarithmic rate law at passive potentials [12]. Xu [13] studied the repassivation behaviour of 316 L stainless steel in a borate buffer solution. They divided the initial current transient into substrate dissolution current and passive film formation current. It was found that the repassivation process is dominated by anodic dissolution only in the initial stages, and that the dissolution current rapidly decays below the film formation current.

CoCrMo alloys are widely used for orthopaedic implants due to their excellent corrosion and wear resistance. In a physiological environment, the presence of proteins and phosphates affect the electrochemical behaviour of the implant and, consequently, affect the depassivation–repassivation process [14–16]. The mechanism of biotribocorrosion is complex and so far there is no clear explanation for it.

In this paper, the depassivation process was investigated in detail. Current variation in the first few cycles under tribological contact in simulated body fluids was recorded and a quantitative relation between depassivation rate (D), applied load (F) and stroke frequency (f) was concluded. The composition change of the oxide film after electrochemical depassivation was analysed by AES.

2. EXPERIMENTAL METHODS AND MATERIALS

2.1 Materials and sample preparation

The forged CoCrMo alloy (ASTM F75–1987) used in this work contained 63% Co, 28% Cr, 5% Mo and 0.2% C (wt. %) (a small amount of Ni, Si, etc.). For tribocorrosion tests, the specimens were 20 mm in diameter and 5 mm in thickness. For AES tests, the specimens were 10 mm in diameter and 3 mm in thickness. The surface of the specimens were wet, ground with SiC paper up to 3000 grit

and then polished with diamond paste. After polishing, the specimens were cleaned in ethanol and distilled water.

2.2 Electrochemical test

The electrolytes used were 0.9% NaCl and 0.9% NaCl with the addition of 10 g L⁻¹ bovine serum albumin (BSA). The three-electrode system included the specimen as the Working Electrode (WE), a platinum wire as the Counter Electrode (CE) and a silver/silver chloride electrode as the Reference Electrode (RE). The tribocorrosion tests were carried out with a UMT-II reciprocating wear tester. The electrochemical station was connected with the wear tester to record current variation during the tribocorrosion process. The applied loads (F) were 2N, 3N and 5N and the stroke frequencies were 0.03 Hz, 0.08 Hz and 0.12 Hz (the corresponding rotating speeds were 2 rec/min, 5 rec/min and 7 rec/min). The sliding distance was 15 mm and the counterpart used was ZrO₂ with a 5 mm diameter. The friction of coefficient was measured one point per second. For potentiodynamic tests, a scan rate of 1 mV/sec was used. The scan range was set from -1.0 V vs. Ag/AgCl to 1.0 V vs. Ag/AgCl.

2.3 Auger electron spectroscopy

AES analysis was carried out by a PHI-700 nanoscanning Auger system. The variation of the elemental composition of the surface oxide layer was analysed in depth. The elemental analysis of Co, Cr, Mo, O and N was performed as a function of sputter time. The sputter rate was 3 nm/min.

3. RESULTS

3.1 Potentiodynamic polarisation measurement

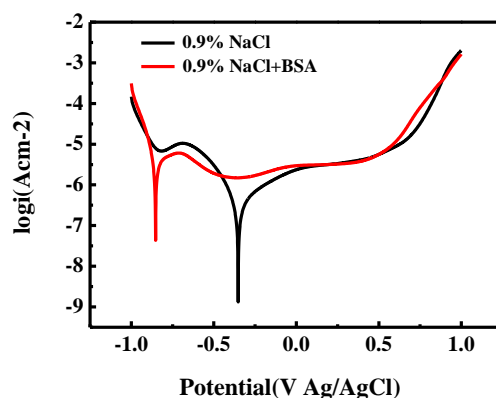


Figure 1. Anodic polarization curve for the CoCrMo alloy in 0.9% NaCl solution and 0.9%NaCl+BSA solution

Potentiodynamic polarisation was conducted to gain information about the electrochemical response of CoCrMo alloys in 0.9% NaCl and 0.9% NaCl + BSA. Fig. 1 indicates that CoCrMo alloys show stable passivity in different solutions. The passive range extends from 0 V to 0.5 V in 0.9% NaCl and -0.5 V to 0.5 V in 0.9% NaCl + BSA. The corrosion current for material in 0.9% NaCl is about $2.1\mu\text{A}$ and in BSA containing solution, it increases to $32\mu\text{A}$. The result indicates that the addition of BSA can enhance the corrosion rate for CoCrMo alloys at static conditions.

3.2 Tribocorrosion tests

A potential within the passive region was applied, and the current variation in the first few cycles was measured as a function of the applied load and stroke frequency. The current variation recorded in different solutions is presented in Fig. 2 and Fig. 3. Corrosion current was kept at a certain range before the start of loading.

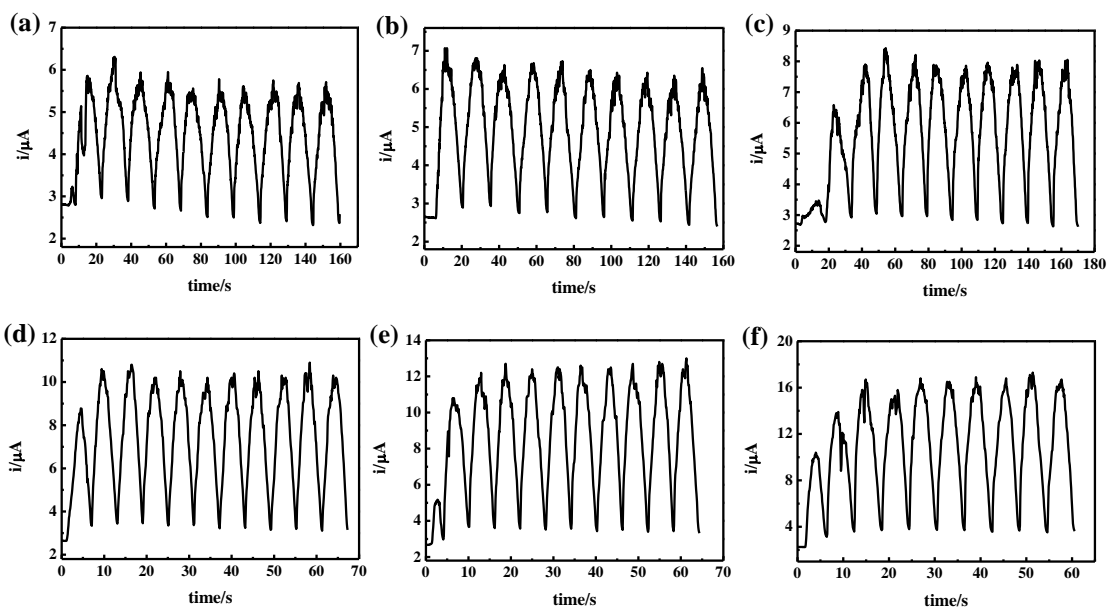


Figure 2. Current as a function of time for the CoCrMo alloy in 0.9%NaCl at an applied potential of 0.2V vs. Ag/AgCl at $f = 0.03\text{Hz}$ and different loads, (a) $F = 2\text{N}$ (b) $F = 3\text{N}$ (c) $F = 5\text{N}$; $f = 0.08\text{Hz}$, (d) $F = 2\text{N}$ (e) $F = 3\text{N}$ and (f) $F = 5\text{N}$

There was an increase in the current, as the stroke started to correspond to the rupture of the surface oxide film, upon which cyclic current variation with time can be seen clearly. The period of current change is related to the stroke frequency and in a single cycle the current increases to maximum at first and then decreases to minimum corresponding to the depassivation–repassivation process. The current reaches its peak value when the sliding velocity is highest and gradually decreases to minimum with sliding velocity decreasing to zero. Thus, the corrosion current mainly affects the surface area of the alloy exposed to the solution instantaneously during the tribocorrosion process.

The current peak is significantly higher in 0.9% NaCl compared with 0.9 % NaCl + BSA under the same mechanical conditions. Fig. 4 shows that friction decreases after the addition of BSA. The

protein adsorption layer may act as a lubricant during the tribocorrosion process, reducing the friction coefficient, thereby, reducing friction, which in turn reduces the corrosion current. In previous studies, the proteins adsorbed to the oxide film created an initial shielding layer on top of the oxide film and made its degradation less drastic [17]. The adsorbed proteins will also hinder the cathodic process by blocking oxidants into the metal surface [18]. These reasons can explain why the current becomes lower when adding BSA.

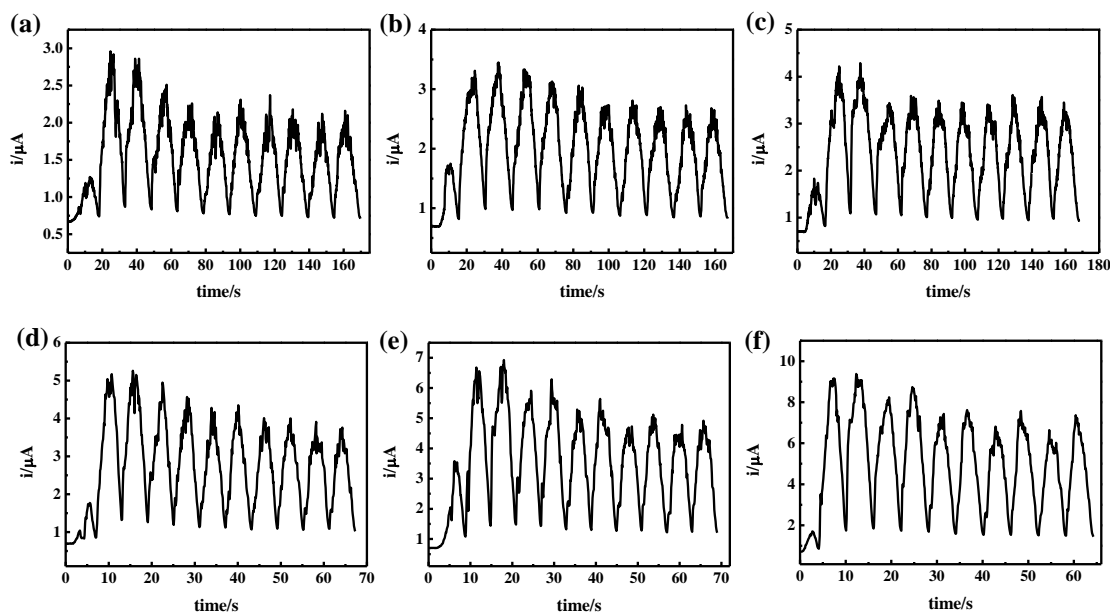


Figure 3. Current as a function of time for the CoCrMo alloy in 0.9%NaCl+BSA at an applied potential of 0.2V vs. Ag/AgCl, at $f = 0.03\text{Hz}$ and different loads, (a) $F = 2\text{N}$ (b) $F = 3\text{N}$ (c) $F = 5\text{N}$; $f = 0.08\text{Hz}$, (d) $F = 2\text{N}$ (e) $F = 3\text{N}$ and (f) $F = 5\text{N}$

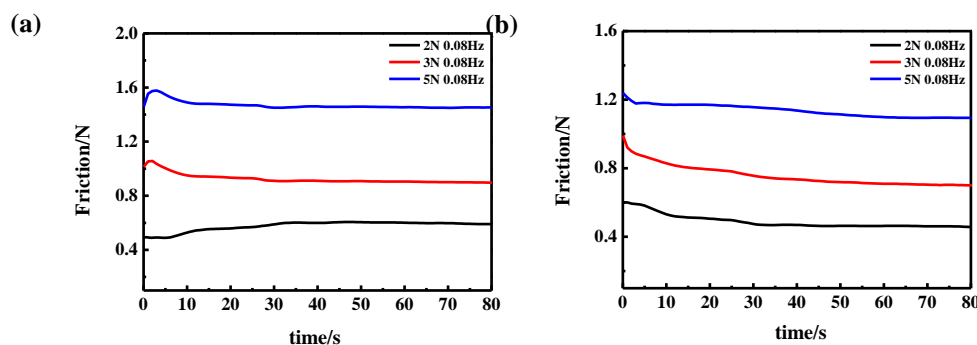


Figure 4. Fictional forces in different solutions (a) 0.9%NaCl+BSA (b) 0.9%NaCl+BSA

For materials used in a tribocorrosion environment, the applied load determines the contact area, while the stroke frequency affects the sliding velocity of the counterpart in an instant. The properties of the passive film, which mainly include structure and composition, will also influence corrosion. All three factors affect the area of the bare alloy exposed to the solution, thus, affecting the

corrosion current. For a given load and stroke frequency, the passive film properties are the main reason affecting corrosion current in different cycles of friction.

Fig. 2 shows that the current peak increases gradually in the first two cycles, becoming steady in later cycles. The results are contrary after adding BSA. Fig. 3 shows that the current is significantly higher in the first two cycles and changes to a lower steady state later. The change of the passive film properties and the adsorption layer are the main factors that affect the corrosion current in different cycles of the tribocorrosion process. The first cycle of friction begins with the initially formed passive film, while the later cycles reflect the properties of re-passivated film. For the solution without proteins, the change of the passive film properties in depassivation–repassivation can explain the current variation. AES was conducted to specify the composition of the oxide film in Fig. 5.

3.3 AES tests

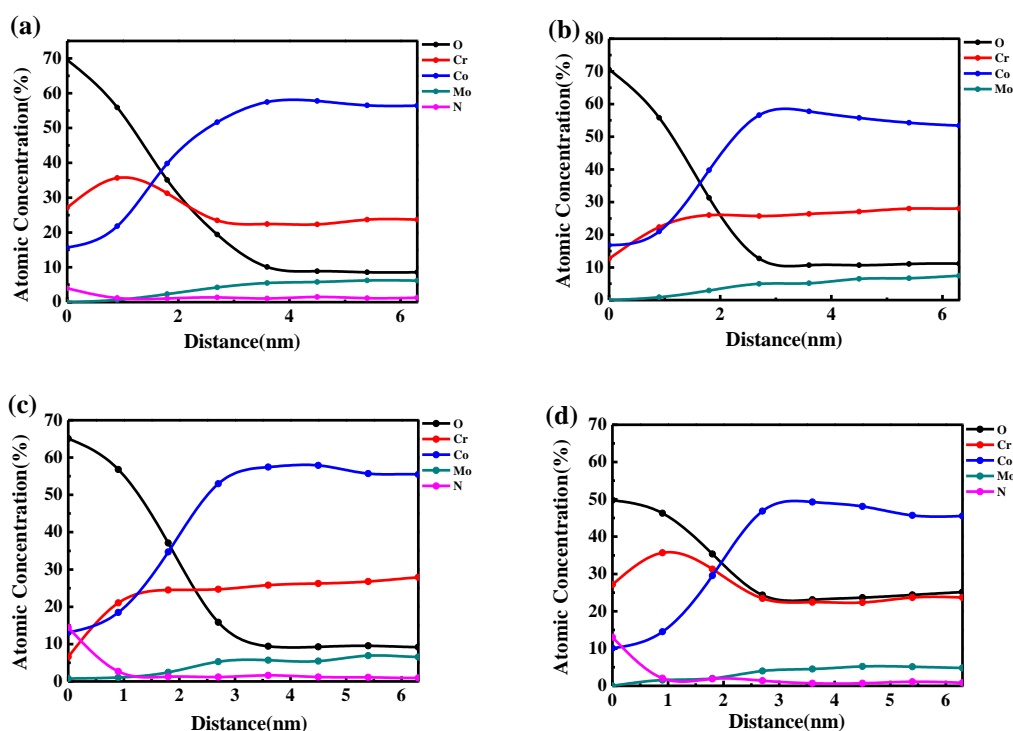


Figure 5. AES depth profiles of samples immersed for 5 hours in (a) 0.9%NaCl at OCP, (b) 0.9%NaCl at 0.2V vs. Ag/AgCl with depassivation (c) 0.9%NaCl+BSA at 0.2V vs. Ag/AgCl with depassivation and (d) 0.9%NaCl+BSA at 0.2V vs. Ag/AgCl without depassivation

The corrosion current in different cycles was compared and proved to have a great difference. It was lower in the first cycle compared with later cycles (relatively stable) in 0.9% NaCl, while the results were contrary in 0.9% NaCl + BSA. According to the analysis above, the change of the passive film properties will have an effect on corrosion in the depassivation–repassivation process. It is difficult, however, to analyse the change of film properties in different cycles of friction. Therefore, the electrochemical method (-0.8 V cathodic potential) was used to remove the original oxide film and the composition of the re-passivated film was analysed. Using this kind of electrochemical method

instead of mechanical forces to achieve depassivation might bring valuable results, although these two methods have differences.

Fig. 5 shows the elemental composition of the surface oxide layer as a function of sputtered depth. There is no significant difference in the oxide film thickness in different testing conditions. Figs. 5 (b) and (c) show the composition of the surface oxide film after electrochemical depassivation under the same potential with and without the addition of BSA. In addition, Figs. 5 (a) and (d) show the composition of oxide film on samples directly immersed in different solutions and potentials. An obvious difference is that the composition of the outer layer oxide film varies significantly depending on whether electrochemical depassivation was performed. The atomic concentration of Cr is significantly higher for samples directly immersed in solution. The reason for this phenomenon could be that the oxide film formed in the air does not dissolve completely in solution. Previous studies have shown that Cr was enriched at the outermost surface oxide after immersion, while Co was reduced due to preferential release [19, 20]. The enrichment and passivation of Cr must result in good resistance for the alloys. Also, because of the short interval time between two successive strokes, the structure of the repassivation film cannot be as compact as the original oxide film. The composition and structure change of the oxide film after depassivation may occur for the current variation in 0.9% NaCl under tribological contact. When BSA is added, however, the adsorption of proteins and the effects of mechanical rolling result in different current variation.

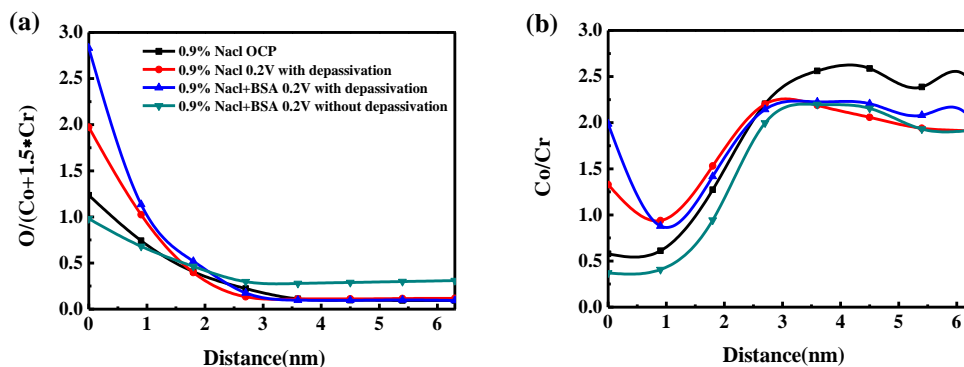


Figure 6. Depth profiles at different testing condition (a) $O/(Co+1.5Cr)$ and (b) Co/Cr

In order to observe more clearly the degree of oxidation of the two main alloying components, Co and Cr, AES data are presented as the ratios of $O/(Co + 1.5 Cr)$ and Co/Cr , as a function of the sputtered depth [21]. In reference to this method, the analysis results are shown in Fig. 6. For the samples with depassivation, the $O/(Co + 1.5 Cr)$ ratio is significantly higher and both ratios decrease in the outer layer oxide film compared with those without depassivation. This indicates that the oxide film formed in the air, which mainly contains Cr_2O_3 and CoO still exists for samples without electrochemical depassivation, while the cobalt oxide in the outer layer is mainly in the form of $CoO/Co(OH)_2$ for the samples with electrochemical depassivation.

4. DISCUSSION

Corrosion resistance of the CoCrMo alloy is related to the formation of a thermodynamically stable passive film which acts as a kinetic barrier to material flow at the interface, thereby reducing corrosion. While in a tribocorrosion environment, corrosion resistance depends on the stability and repassivation ability of the passive film. Wear-accelerated corrosion can be limited greatly if the alloy can recover its passive state quickly after the passive film is destroyed. In a saline solution, the corrosion current increases along with charge transfer when the passive film is destroyed, while the film is reformed after depassivation prevents further oxidation of the alloy. The depassivation-repassivation phenomenon has been recognized previously for passive alloys such as stainless steels, Ti alloys and so on [10, 22-24]. In literature, initially the depassivation and repassivation are both related to electrochemical processes [11]. However, mechanical force is another factor which has a greater influence to the depassivation process [1, 10]. For hip or knee implants, the effect of proteins to the depassivation-repassivation is really important as the longevity and safety of such medical devices rely on the stability of the material surface. Micro-indentation experiments were carried out by Yamamoto and colleagues [10, 22]. It was found that the passive film rupture was caused by plastic deformation and the charge transfer occurred even during the stress relaxation period.

In order to have a more clear understanding of the relation between the depassivation rate (D), applied load (F) and stroke frequency (f), analysis of corrosion current variation with displacement at the third or fourth cycle of friction was conducted in Fig. 7.

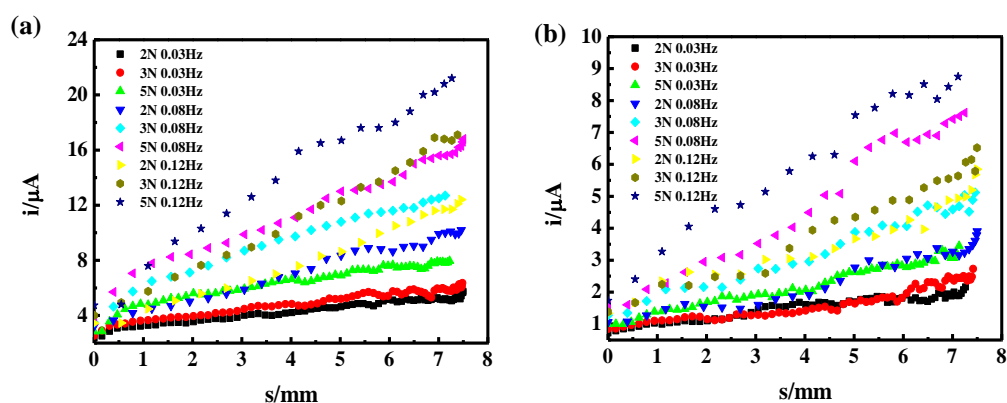


Figure 7. i - s curves in a single depassivation process at the applied potential of 0.2V vs. Ag/AgCl under different load and frequency: (a) 0.9%NaCl and (b) 0.9%NaCl+BSA

The corrosion current changes linearly with displacement, and after linear fitting the calculated slope was defined as the depassivation rate. After non-linear surface fitting, the relation between the depassivation rate, applied load and stroke frequency was deduced. This can be summarised as $D = 7.57E-6F^{0.56}f$ for 0.9% NaCl and $D = 2.31E-6F^{0.85}f$ for 0.9% NaCl + BSA. In Yamamoto's indentation work [10], the maximum current that iron sample could reach at 5 N was about 0.4 μ A. However,

when frictional forces existed, the passive film need to resist the normal load and the frictional force. In our tests, it can be concluded that the frequency (the effect of the frictional force) provided greater effect on the depassivation process than the normal load.

When adding BSA, the adsorption of proteins or the reaction with metal ions through chelating can affect the corrosion behaviour of alloys. Under dynamic tribocorrosion conditions, proteins affect the breakdown of the passive film, the release of metal ions and the repassivation of the film. The protein adsorption layer acts as a lubricant during the tribocorrosion process, reducing friction, which in turn reduces the destruction of the oxide film. In literature, there are a number of papers discussing the effect of proteins on the depassivation process [1, 9]. However, quantitative results of the effect on the frequency and the applied load were few. In addition, the key period which can influence the resistance of surface to tribocorrosion is the initial a few cycles. The alteration of the surface film from spontaneously forming in air to regeneration in electrolyte not only shows on chemical compositions but also on the mechanical properties. Therefore, in this study we focused on the beginning of wear-corrosion processes.

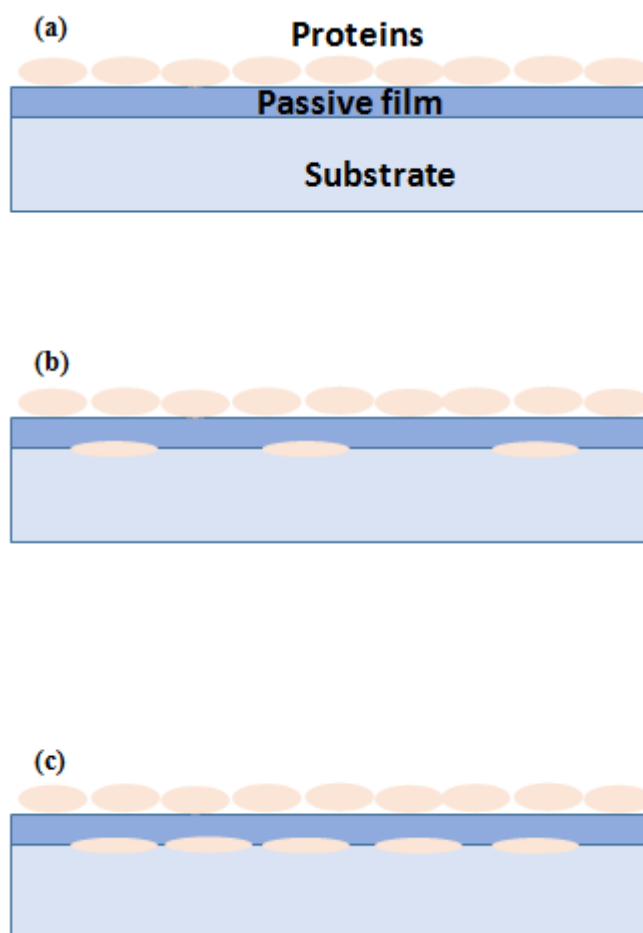


Figure 8. Schematic diagrams of surfaces evolution in tribocorrosion tests (a) original passive film and adsorption layer (b) after a few cycles of friction (c) after a long period of friction

The adsorbed proteins will also impede corrosion reactions by blocking the diffusion of oxygen into metal surfaces. During the depassivation–repassivation process, the film reformed was confirmed

to be different. The passive film was more resistant in the environment containing chloride ions, as the chromium content in the passive film increased. Thus, the decrease of chromium content in depassivated films could result in a higher corrosion current. When BSA was added (Fig. 8), however, the protein adsorption layer was deformed under mechanical wear. The deformed proteins, which sometimes contain ruptured passive film, adhered to the wear track resulting in a lower corrosion current.

5. CONCLUSION

Electrochemical techniques (polarisation and i-t curve), wear tests and surface analysis (AES) were conducted to investigate the depassivation–repassivation kinetics of CoCrMo alloys under tribological contact in simulated body fluids. From the obtained results, the following conclusions are drawn:

- The depassivation rate is related to the applied load and the rubbing frequency. This can be summarised as $D = 7.57E-6F^{0.56f}$ for the tested CoCrMo alloy in 0.9% NaCl solution and $D = 2.31E-6F^{0.85f}$ for BSA containing 0.9% NaCl solution.

- The change of passive film properties during the depassivation–repassivation process was analysed. It was found that the ratio of the Cr element in the outer layer of the passive film was lower after repassivation. The passive film formed initially has better stability, which results in a lower depassivation rate in the first few cycles compared with later cycles (relatively stable) in 0.9% NaCl. The adsorption of BSA and the effects of mechanical rubbing result in a higher depassivation rate in the first two cycles in 0.9% NaCl + BSA.

ACKNOWLEDGEMENT

Financial support to this work from the National Key Technology R&D Program 2014BA11B04 is greatly acknowledged.

References

1. Y. Yan, D. Dowson and A. Neville, *J. Mech. Behav. Biomed. Mater.*, 18 (2013) 191.
2. J. Jiang and M.M. Stack, *Wear*, 261 (2006) 954.
3. K. Fushimi, T. Shimada, H. Habazaki, H. Konno and M. Seo, *Electrochim. Acta*, 56 (2011) 1773.
4. M. Seo and Y. Kurata, *Electrochim. Acta*, 48 (2003) 3221.
5. M. Seo and M. Chiba, *Electrochim. Acta*, 47 (2001) 319.
6. M. Chiba and M. Seo, *Electrochim. Acta*, 50 (2004) 967.
7. P. Ghods, O. Burkan Isgor, F. Bensebaa and D. Kingston, *Corr. Sci.*, 58 (2012) 159.
8. A.W.E. Hodgson, S. Kurz, S. Virtanen, V. Fervel, C.O.A. Olsson and S. Mischler, *Electrochim. Acta*, 49 (2004) 2167.
9. D. Landolt, S. Mischler and M. Stemp, *Electrochim. Acta*, 46 (2001) 3913.
10. T. Yamamoto, K. Fushimi, M. Seo, S. Tsurii, T. Adachi and H. Habazaki, *Corr. Sci.*, 51 (2009) 1545.

11. C. Olsson, D. Hamm, D. Landolt, C. Olsson and D. Hamm, *J. Electrochem. Soc.*, 147 (2000) 4093.
12. F.J. Graham, H.C. Brookes and J.W. Bayles, *J. Appl. Electrochem.*, 20 (1990) 45.
13. H. Xu, D. Sun and H. Yu, *Appl. Surf. Sci.*, 357 (2015) 204.
14. Y. Yan, A. Neville, D. Dowson and S. Williams, *Tribol. Int.*, 39 (2006) 1509.
15. A.I. Mun Oz and S. Mischler, *J. Electrochem. Soc.*, 154 (2007) C562.
16. A.C. Lewis, M.R. Kilburn, I. Papageorgiou, G.C. Allen and C.P. Case, *J. Biomed. Mater. Res. Part A*, 7 (2005) 456.
17. M.J. Runa, M.T. Mathew, M.H. Fernandes and L.A. Rocha, *Acta Biomater.*, 12 (2015) 341.
18. C. Valero Vidal, A. Olmo Juan and A. Igual Muñoz, *Colloid Surf. B-Biointerfaces*, 80 (2010) 1.
19. K. Yamanaka, M. Mori and A. Chiba, *Acta Biomater.*, 31(2016) 435.
20. Y. Hedberg and I.O. Wallinder, *J. Biomed. Mater. Res. Part B*, 102 (2013) 693.
21. M. Behazin, J.J. Noël and J.C. Wren, *Electrochim. Acta*, 134 (2014) 399.
22. T. Yamamoto, K. Fushimi, H. Habazaki and H. Konno, *Electrochim. Acta*, 55 (2010) 1232.
23. T.O. Nagy, U. Pacher, A. Giesriegl, L.Soyka, G. Trettenhahn and W. Kautek, *Appl. Surf. Sci.*, 302 (2014) 184.
24. P. Henry, J. Takadoum and P. Bercot, *Corr. Sci.*, 53 (2011) 320.

© 2017 The Authors. Published by ESG (www.electrochemsci.org). This article is an open access article distributed under the terms and conditions of the Creative Commons Attribution license (<http://creativecommons.org/licenses/by/4.0/>).